Spintronic single-qubit gate based on a Π-shaped lateral quantum dot with spin-orbit interaction

S. Bellucci[1] and P. Onorato[1,2]
[1]*Laboratori Nazionali di Frascati, INFN, P.O. Box 13, 00044 Frascati, Italy*
[2]*Dipartimento di Ingegneria dell'Informazione, Seconda Università di Napoli, 81031 Aversa (CE), Italy*
(Received 22 July 2008; revised manuscript received 6 November 2008; published 23 January 2009)

In a quantum nanometric lateral quantum dot (QD) with a Π geometry the spin properties of a single electron injected in the Coulomb blockade regime are modified by the spin-orbit interaction, resulting in a transformation of the qubit state carried by the spin. The Π-shaped QD acts as a one-qubit spintronic quantum gate whose properties can be varied by tuning the Rashba parameter of the spin-orbit interaction, by changing the relative position of the junctions, as well as by modifying the length of the transverse legs. We discuss how a large class of transformations can be attained with already one Π nanojunction or a few Π nanojunctions in series.

DOI: 10.1103/PhysRevB.79.045314 PACS number(s): 72.25.−b, 72.20.My, 73.50.Jt

I. INTRODUCTION

Because the spin degree of freedom promises many applications in electronics,[1,2] recently, increasing attention, from both experimental and theoretical physics communities, has been devoted toward the interplay of spin-orbit interaction (SOI) and quantum interference effects in confined semiconductor heterostructures. Such interplay can be exploited as a means to control and manipulate the spin degree of freedom at a mesoscopic scale useful for phase-coherent spintronic applications.[1]

In general, the SOI can be described by the Hamiltonian[3]

$$\hat{H}_{\mathrm{SO}} = -\frac{\lambda_0^2}{\hbar} m_0 e \mathbf{E}(\mathbf{r}) \cdot [\hat{\sigma} \times \hat{\mathbf{p}}]. \tag{1}$$

Here $\mathbf{E}(\mathbf{r})$ is the electric field, $\hat{\sigma}$ are the Pauli matrices, $\hat{\mathbf{p}}$ is the canonical momentum operator, $\mathbf{r}$ is a three-dimensional (3D) position vector, $\lambda_0^2 = \hbar^2/(2m_0c)^2$, and m_0 is the electron mass in vacuum, while in materials m_0 and λ_0 are substituted by their effective values m^* and λ. The SO term can be seen as the interaction of the electron spin with the magnetic field B_{eff} appearing in the rest frame of the electron.

In this paper we focus on a low-dimensional nanostructure patterned in a two-dimensional electron gas (2DEG), a gas of electrons free to move in two dimensions, but tightly confined in the third. This tight confinement leads to quantized energy levels for motion in that direction, which can then be ignored for most problems. In order to engineer a 2DEG, it is usual to utilize the heterojunction between two semiconducting materials which confines electrons into a triangular quantum well. Thus, due to the band offsets at the interface of two different materials, electrons are confined by forming a 2DEG (in the xy plane), while because of the asymmetry in the quantum well potential that confines the 2DEG,[4] the electrons are moving in an effective electric field E_z along $\hat{z}$. The Rashba SOI (Ref. 5) stems from the discussed structure inversion asymmetry of the heterostructure quantum well. However, in 2DEGs, there are also different types of SOI: the Dresselhaus term which originates from the inversion asymmetry of the zinc-blende structure and the confining β-coupling term arising from the in-plane electric potential that is applied to squeeze the 2DEG into a defined nanostructure.[6] Since the original proposal of the spin field-effect transistor by Datta and Das,[7] many proposals appeared based on intrinsic spin-splitting properties of semiconductors associated with the Rashba SOI. This is a dominant mechanism that has been proven to be a convenient means for achieving an all-electrical control of the spin-polarized current through additional gate voltages. Recent measurements based on the spin-galvanic effect provided the magnitude of the ratio of Rashba and Dresselhaus[8] terms. This ratio can reach values as large as 2.14 ± 0.25 in InAs quantum wells.[9] The Rashba term is in general dominant but the Dresselhaus interaction can yield observable effects.

The Rashba Hamiltonian obtained from Eq. (1) takes the form[6]

$$\hat{H}_{\mathrm{SO}}^{\alpha} = \frac{\alpha}{\hbar}[\sigma_x p_y - \sigma_y p_x] = \frac{\hbar k_R}{m^*}[\sigma_x p_y - \sigma_y p_x], \tag{2}$$

where α, which in vacuum is given by $\lambda_0^2 E_z e$, in semiconductor heterostructures takes values typically[10–12] within the range of $\sim 10^{-11} - 10^{-12}$ eV m, while its highest value is close to 10^{-10} eV m as reported in Refs. 13 and 14. Here $k_R \equiv \frac{m^*\alpha}{\hbar^2} = \frac{\pi}{L_{\mathrm{so}}}$, which has a natural value[6,15] $k_R \sim 10^{-5} - 10^{-2}$ nm^{-1} for $\alpha \sim 10^{-12} - 10^{-10}$ eV m. The spin-precession length[7] L_{so} measures the strength of Rashba spin splitting[5] in terms of a length scale.

Even though the Rashba spin splitting is expected to be very small, nonetheless this perturbation can give rise to a sizeable modification of a semiconductor band structure.[16,17] Moreover, for applications it is essential that the strength of the Rashba effect, and thus the spin splitting, can be controlled by means of a gate electrode.

The Dresselhaus Hamiltonian takes the form[18]

$$\hat{H}_{\mathrm{SO}}^{\alpha_D} = \frac{\alpha_D}{\hbar}[\sigma_x p_x - \sigma_y p_y] = \frac{\hbar k_D}{m^*}[\sigma_x p_x - \sigma_y p_y], \tag{3}$$

where $\alpha_D \sim \alpha_R/2$.

Prominent experiments have shown injection of spin-polarized currents into semiconductor material,[19] long spin dephasing times in semiconductors (approaching microseconds),[20] ultrafast coherent spin manipulation,[21] as well as phase-coherent spin transport over distances of up to

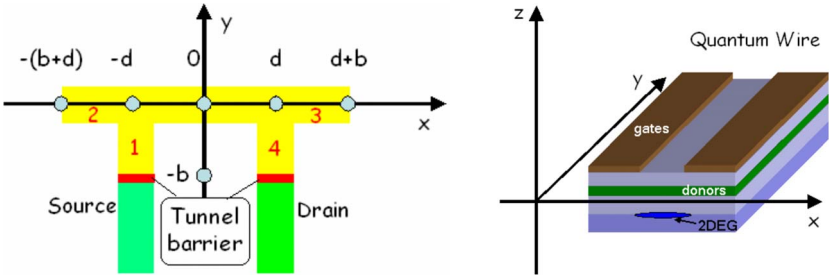

FIG. 1. (Color online) (Left) The Π junctions (Π) can be assumed as crossing junctions involving three Q1D wires of width W ranging between ~25 and 100 nm. Arms 1 and 4 are connected to the contact lead [source (S) and drain (D)] that we suppose to be also ferromagnetic. The current flows through a tunnel junction (S-Π-D) giving a series of events in which exactly one electron passes (tunnels) through the tunnel barriers (single electron tunneling). The two potential barriers at $y=-b$ and $x=\pm d$ can be produced, e.g., by the presence of two quantum point contacts which make the conducting channel narrower, or they could be due to the subband mismatch between the junction and the external leads. (Right) Schematic of a quantum wire patterned in a 2DEG obtained at the interface of a semiconductor heterostructure. In these devices we can consider that the degree of freedom corresponding to z is quantum mechanically frozen out.

100 μm.[20] Irrespective of spin, the charge of the electrons can be used to control single electrons by confining them in quantum dot (QD) structures, leading to striking effects in the Coulomb blockade (CB) regime.[22]

In addition, suitable means for controlling spin at mesoscopic scales are provided by quantum interference effects. The effects of spin interference caused by Rashba SOI were largely studied in the last years, and more recently they were measured experimentally. In Ref. 23 the authors studied Aharonov-Bohm-type conductance oscillations in ring structures as a function of the Rashba-SOI strength and associated these observations with the Aharonov-Casher (AC) effect.

In a recent paper[24] the spin rotation due to the Rashba SOI induced by the spin interference in a ballistic quasi-one-dimensional (Q1D) Π nanojunction, a crossing junction involving three Q1D wires (Fig. 1) with two leads was analyzed. This device, such as the quantum ring in Ref. 25, acts as a one-qubit spintronic quantum gate whose properties can be varied by tuning the Rashba parameter of the SOI. However, in the discussed structures, it is very difficult to handle a single electron, while one has to handle a single electron for quantum information processing because information is carried by the spin of a single electron. It follows that the customary continuous transport experiment cannot be utilized as quantum information processing. Thus, here, our aim is to find a device which works in a different regime rather than in the ballistic one, where a single electron spin can be handled by obtaining the same kind of spin rotation.

Thus in this paper we focus on the single electron transport in the Π nanojunction subject to Rashba SOI and show that this device made of a semiconductor structure such as InGaAs, in which Rashba-type SOI is the dominant spin-flipping mechanism, can render a one-qubit spintronic quantum gate. In this case we assume that the device works in the Coulomb blockade regime and can be assumed as an empty lateral QD. We show that also in this regime, where the quantized energy levels of the isolated Π junction are involved, the system acts as a spin rotator and operates as a spintronic quantum gate acting on a single electron. Thus we assume that two tunnel barriers, as shown in Fig. 1 (left), are now introduced between the external leads (source and drain) and the Π nanojunction. These potential barriers introduced in the model could be due to the presence of two quantum point contacts by introducing a weak coupling between the external leads and the device (see, e.g., Ref. 26). Obviously the approach used in the ballistic regime has to be modified and replaced by a suitable formalism in order to describe the single electron tunneling.

In this paper we first analyze the model which describes the suggested device by calculating the relevant parameters in the physics of Q1D ballistic devices. Next we calculate the single-particle energy levels obtained applying the quantum waveguide approach and discuss the spin polarization of the corresponding eigenstates. Starting from the knowledge of the electron bound states we will be able to study the behavior of a single electron injected in the Π QD, and we will analyze that from a spintronics point of view.

II. SOI IN Q1D SYSTEMS AND WAVE FUNCTIONS

The quasi-one-dimensional ballistic quantum wire (QW), a nanometric solid-state device, is the basic building block of the considered nanojunction. In the QW the transverse motion is quantized into discrete modes, and the longitudinal motion is free. In this case, electrons propagate freely down a clean narrow pipe, and electronic transport with no scattering can occur.

If we assume that the QW is oriented along the y axis, as in Fig. 1 (right), and the lateral confining potential $V_c(x)$ is approximated by a parabola[27] [where ω is related to the effective width W of the QW according to the formula $2W^2=\hbar/(m^*\omega)$], thus the Hamiltonian without the SOI reads

$$\hat{H}_0 = \frac{\mathbf{p}^2}{2m^*} + V_c(\mathbf{r}) = \frac{\mathbf{p}^2}{2m^*} + \frac{m^*}{2}\omega^2 x^2. \tag{4}$$

As we know from Refs. 28 and 29, the QW Hamiltonian in the presence of Rashba SOI cannot be exactly diagonalized. Thus Hamiltonian (3) can be separated in a commuting part ($[\hat{H}_c,\hat{H}_0]=0$)

$$\hat{H}_c = \frac{1}{\hbar}(\alpha\hat{\sigma}_x + \alpha_D\hat{\sigma}_y)p_y = \frac{\hbar\tilde{k}_R p_y}{m^*}\hat{\tilde{\sigma}}_x, \tag{5}$$

and a nondiagonal part.[28,29]

In the presence of a significant Dresselhaus SOI we redefine the quantization axis for the spin by introducing

$$\hat{\tilde{\sigma}}_x = \frac{\alpha\hat{\sigma}_x + \alpha_D\hat{\sigma}_y}{\sqrt{\alpha^2+\alpha_D^2}}$$

and $\tilde{k}_R = \sqrt{\alpha^2+\alpha_D^2}/\alpha$.

It follows that the Rashba subbands splitting in the energies, in the first-order approximation, read

$$\varepsilon_{n,k,s_x} = \hbar\omega\left(n+\frac{1}{2}\right) + \frac{\hbar^2}{2m^*}[(k \pm k_R)^2 - k_R^2]. \quad (6)$$

The ± sign corresponds to the spin polarization along the x axis, i.e., to the spin eigenstate χ_{s_x}, while the confining energy $\hbar\omega$ can be also read as the intersubband gap.

If we also include in the calculation the Dresselhaus term we have to replace in Eq. (6) k_R with $\tilde{k}_R$ while the spin is now polarized with respect to a new axis $\tilde{x}$ forming an angle $\tilde{\theta}$ with the x direction, where $\tan(\tilde{\theta}) = \frac{\alpha_D}{\alpha}$.

The noncommuting term can be neglected in the first-order approximation and becomes relevant just near the crossing points $k = \pm k_c = \frac{\omega m^*}{\hbar k_R}$, as was discussed in Refs. 28 and 29 and bibliographies therein. Thus, as we easily obtain from Eq. (6), the approximation is largely justified for values of the energies below

$$\varepsilon_c = \hbar\omega\left(1+\frac{L_{\mathrm{SO}}^2}{4W^2}\right).$$

Hence we can conclude that four-split channels are present for a fixed Fermi energy ε_F, corresponding to $\pm p_y$ and $s_x = \pm 1$ (or $\tilde{s}_x = \pm 1$ if we also include α_D) with eigenfunctions

$$f_{\varepsilon_F,n,s_x} = u_n(x)e^{ik_n^s(\varepsilon_F)y}\chi_{s_x},$$

where $u_n(x)$ are harmonic-oscillator eigenfunctions. Here

$$k_n^s(\varepsilon_F) = sk_R \pm \sqrt{k_R^2+k_n^2} \equiv sk_R \pm q_n,$$

where $k_n^2 = \frac{2m^*}{\hbar}(\varepsilon_F - \hbar\omega\frac{2n+1}{2})$ and $q_n = \sqrt{k_R^2+k_n^2}$.

The QW Hamiltonian in general has eigenfunctions belonging to the one-dimensional (1D) subbands ($n=0,1,\ldots$); however in the Q1D limit we can assume $n=0$ and neglect the transverse part of the wave function $u_n(x)$. The latter approximation can be justified by assuming the energy of the lowest levels in the QD, or more in general the Fermi energy in the leads, to be less than $3\hbar\omega/2$ corresponding to the bottom of the $n=1$ subband. In the following we will refer to a QW with an effective width of $W\sim 20$ nm where $\hbar\omega \sim 50$ meV, while the lowest energy levels are below 60 meV.

III. Π JUNCTION

In order to obtain the single-particle spectrum of the Π QD we use the one-dimensional quantum waveguide theory.[30] This approximation is justified if we assume (i) the effective width, W, to be smaller than the other length parameters (b,d) and (ii) the energy of the lowest energy levels ε to be smaller than $3\hbar\omega/2$. The latter condition, discussed above, can be replaced when we define the rescaled energy $\tilde{\varepsilon} = \varepsilon - \hbar\omega/2$ that has to be smaller than the intersubband gap, $\hbar\omega$, i.e., the energy gap between the bottom of two nearest subbands.

If these conditions are fulfilled, the transverse dimension is negligible and we can treat the junction as a strictly one-dimensional device and neglect the contribution of $u_n(x)$. Thus, in each of the four QWs, the Hamiltonian $H_0 + H_c^\alpha$ has eigenfunctions belonging to the lowest 1D subband $n=0$ given by

$$f_{q,\rightarrow}^{\parallel} = e^{iqy}e^{ik_Ry}\chi_{\rightarrow}^x, \quad f_{q,\leftarrow}^{\parallel} = e^{iqy}e^{-ik_Ry}\chi_{\leftarrow}^x,$$

$$f_{q,\uparrow}^{=} = e^{iqx}e^{ik_Rx}\chi_{\uparrow}^y, \quad f_{q,\downarrow}^{=} = e^{iqx}e^{-ik_Rx}\chi_{\downarrow}^y,$$

where $\parallel$ stands for probes 2, 5, or 3 and $=$ for sectors 1 and 4.

IV. ENERGY LEVELS

First of all, we introduce the wave functions, ψ_p, in each of the five different regions: the bottom arms 1 and 4, the interferometric region ($-d<x<d$), and the two side arms 2 and 3. Notice that the arms are closed, i.e., $\psi_2[-(d+b),0] = 0$ and $\psi_3(d+b,0)=0$, while $\psi_1(-d,-b)=0$ and $\psi_4(d,-b) = 0$ (the latter condition corresponds to assume an infinite potential barrier at $y=-b$, i.e., to consider the limit of weak coupling between the external leads and the device). Thus we use the Griffith[31] boundary condition, which states that the wave function is continuous in $(-d,0)$ and $(d,0)$, and that the current density is conserved at each intersection. The resulting set of linear equations leads to a relation between the expansion coefficients A_q^σ in the different domains and also yields the allowed energies for the quantum system.

The values of q_n corresponding to the allowed energy levels are obtained by the solution of

$$\cot(q_nd) = \frac{1}{2}\tan(q_nb), \quad \text{symmetric (S)}, \quad (7)$$

$$\tan(q_nd) = -\frac{1}{2}\tan(q_nb), \quad \text{antisymmetric (A)}, \quad (8)$$

$$\sin(q_nb) = 0 \quad \text{(GS)}. \quad (9)$$

Notice that the energy levels do not depend on the strength of SOI and are fixed just by the size of the Π junction as shown in Fig. 2.

Now we want to discuss the energy levels for three different geometries of the Π dot. Here we suppose $\hbar\omega \sim 50$ meV corresponding to $W\sim 20$ nm and $\frac{\hbar^2\pi^2}{2m^*b^2} \sim 20$ meV, corresponding to $b=100$ nm.

If we assume $b=d\sim 100$ nm (A junction in Fig. 2) we obtain the energy levels for $q_m \sim (0.3+\frac{m}{2})\frac{\pi}{b}$ (S), for $q_m \sim (\frac{m+1}{2})\frac{\pi}{b}$ (A), and for $q_m \sim (m+1)\frac{\pi}{b}$ according to Eqs. (7)–(9). Thus the ground state (GS) (S) corresponds to $\tilde{\varepsilon}_q \sim 1$ and 8 meV while the first excited state (A) corresponds to $\tilde{\varepsilon}_q \sim 5$ meV.

If we assume $d=2b\sim 200$ nm (B junction in Fig. 2) we obtain the energy levels for $q_m \sim (0.2+\frac{m}{2})\frac{\pi}{b}$ (S), for q_m

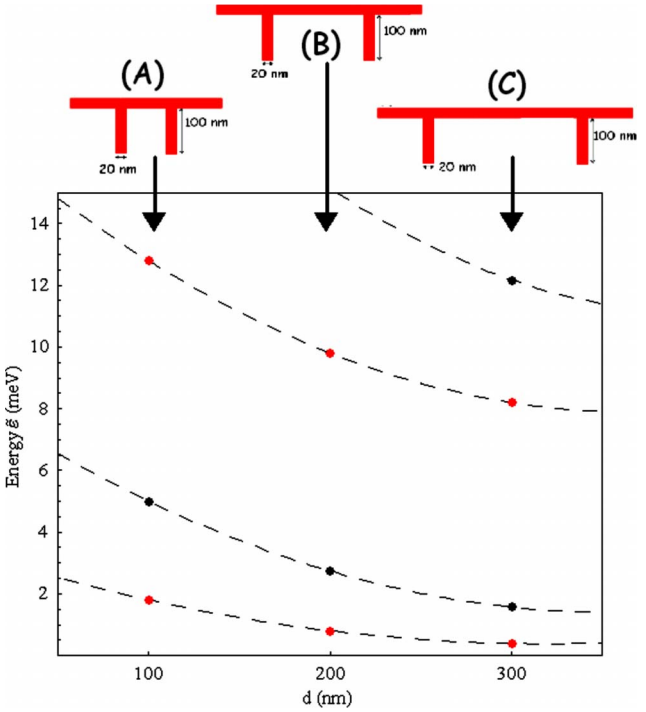

FIG. 2. (Color online) The energy spectra for different geometries (i.e., as a function of the constructive parameters d and b). The lowest energy levels as a function of the interferometric distance, d, for a fixed length of the arms ($b=100$ nm). We report the rescaled energy $\tilde{\varepsilon}$ in meV.

$\sim(0.37+\frac{m}{2})\frac{\pi}{b}$ (A), and for $q_m\sim(m+1)\frac{\pi}{b}$. Thus the GS (S) corresponds to $\varepsilon_q\sim 0$ and 8 meV, while the first excited state (A) corresponds to $\tilde{\varepsilon}_q\sim 2$ and 7 meV.

If we assume $d=3b\sim 300$ nm (C junction in Fig. 2) we obtain the energy levels for $q_m\sim(0.14+\frac{m}{2})\frac{\pi}{b}$ (S), for $q_m\sim(0.28+\frac{m}{2})\frac{\pi}{b}$ (A), and for $q_m\sim(m+1)\frac{\pi}{b}$. Thus the GS (S) corresponds to $\varepsilon_q\sim 0$ and 4 meV, while the first excited state (A) corresponds to $\tilde{\varepsilon}_q\sim 1$ and 5 meV.

With the aim of engineering a device operating in the Coulomb blockade regime, we have to take into account also the electron-electron repulsion and the thermal effects. The Coulomb repulsion, U_c, that has to be taken into account when a second electron is injected in the dot is $U_c \gtrsim 1$ meV [of the same order as the energy gap Δ between the GS and the first excited level]. Moreover the thermal energy can be evaluated as $k_B=8.6\times 10^{-2}$ meV K^{-1}; hence the gap of 1 meV is observable up to a temperature about 10 K. Thus, in the following we suppose that the QD is empty and neglect the effect of a second electron injected.

V. SPIN-POLARIZED INJECTION IN THE Π QD

Next we suppose that the QD is empty. Obviously the discussion can be extended to a many-electron dot by including the effect of the spin-dependent electron-electron interaction.[32] Thus we can limit ourselves to the ground state of the QD.

Nevertheless the spin degeneration of the eigenstates requires the knowledge of the spin polarization in one of the arms. If we suppose that the injected electron comes from a ferromagnetic source (i.e., spin polarized) contact, we can also fix the spin polarization in arm 1 (see Fig. 3, top) near the tunnel barrier at the lead-dot junction. In fact, in the language of the single-particle picture each level of the QD, m, will have a coupling Γ_m^S (Γ_m^D) due to the different overlap of its wave function with source (drain) contact. Thus we can assume as a boundary condition that the electron in arm 1 and at $y=-d$ is polarized exactly as in the ferromagnetic source (see Fig. 3, top). Starting from this ansatz the spin polarization is univocally defined in all the other regions of the QD.

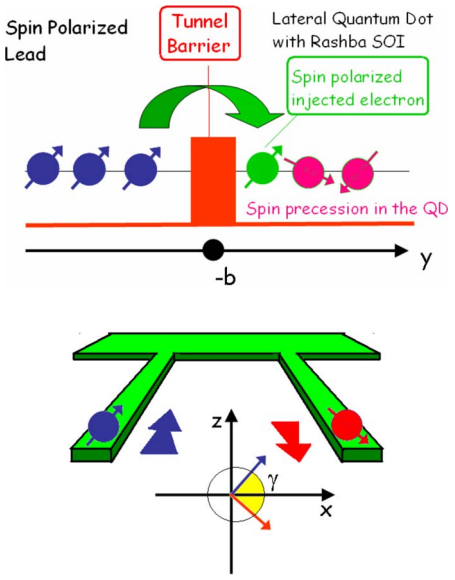

FIG. 3. (Color online) (Top) Spin polarization near the lead-dot junction. (Bottom) Spin rotation around the y axis induced by the combined effect of interference and SOI.

VI. QUBIT OPERATIONS

The π nanojunction proposed here allows for a significant class of spin transformations to be described now in the fixed S_x basis, which is more suitable to discuss the qubit operations in this case. We focus here on the transmission properties of the Π QD when in probe 1 an electron with a generic spin polarization at $y=-b$ is injected,

$$\chi_0 = f^{\rightarrow}\chi_{\rightarrow} + f^{\leftarrow}\chi_{\leftarrow} = \cos\left(\frac{\vartheta}{2}\right)e^{-i\varphi/2}\chi_{\rightarrow} + \sin\left(\frac{\vartheta}{2}\right)e^{i\varphi/2}\chi_{\leftarrow}.$$

Here φ and ϑ are the spherical coordinates which we need in order to describe the spin orientation in the 3D space. χ_0 corresponds to a wave function in arm 1,

$$\psi_1(y) = f^{\rightarrow}e^{ik_R(y+b)}\sin[q(y+b)]\chi_{\rightarrow} + f^{\leftarrow}e^{-ik_R(y+b)}\sin[q(y+b)]\chi_{\leftarrow},$$

which gives

$$\langle S_x\rangle = \cos(\vartheta),$$

$$\langle S_y\rangle = \sin(\vartheta)\cos[\varphi - 2k_R(y+b)],$$

$$\langle S_z \rangle = \sin(\vartheta)\sin[\varphi - 2k_R(y+b)],$$

with the special case of the spin-polarized electrons along the x direction ($f^{\rightarrow}=0$ or $f^{\leftarrow}=0$) where the spin polarization is uniform along all the arms.

The wave function in arm 4 can be written as

$$\psi_4(y) = t^{\rightarrow} e^{ik_R(y+b)} \sin[q(y+b)]\chi_{\rightarrow} + t^{\leftarrow} e^{-ik_R(y+b)} \sin[q(y+b)]\chi_{\leftarrow},$$

where

$$\begin{pmatrix} t^{\rightarrow} \\ t^{\leftarrow} \end{pmatrix} = \begin{pmatrix} U_{14}^{\rightarrow\rightarrow} & U_{14}^{\rightarrow\leftarrow} \\ U_{14}^{\rightarrow\rightarrow} & U_{14}^{\rightarrow\rightarrow} \end{pmatrix} \begin{pmatrix} f^{\rightarrow} \\ f^{\leftarrow} \end{pmatrix} = \mathbf{U}\cdot\mathbf{f}, \tag{10}$$

where $\mathbf{U}$ is a unitary, unimodular matrix which performs a nontrivial spin transformation in the qubit space,

$$\mathbf{U} = \begin{pmatrix} \cos(2k_R d) & i\sin(2k_R d) \\ i\sin(2k_R d) & \cos(2k_R d) \end{pmatrix}. \tag{11}$$

Notice that the transformation given by Eq. (11) is independent of the wave vector q, and it rotates the spin. In fact, the $\mathbf{U}$ matrix acts on χ_0 (ψ_1) by giving in lead 4

$$\langle S_x \rangle = \cos(\gamma)\cos(\vartheta) - \sin(\gamma)\sin(\vartheta)\sin[\varphi - 2k_R(y+b)],$$

$$\langle S_y \rangle = \sin(\vartheta)\cos[\varphi - 2k_R(y+b)],$$

$$\langle S_z \rangle = \sin(\gamma)\cos(\vartheta) + \cos(\gamma)\sin(\vartheta)\sin[\varphi - 2k_R(y+b)].$$

Thus, assuming the injected spin in $y=-b$, with a spin polarization $\langle \vec{S}_0 \rangle$, the Π QD rotates the spin along the x and z axes around the y axis (see Fig. 3) by an angle

$$\gamma \equiv 2k_R d. \tag{12}$$

As was shown in Fig. 2 of Ref. 24, by changing the strength of the SOI (k_R) or the distance $2d$ between the junctions, according to the equation above, the value of γ can be varied.

Notice that the rotation reported in Eq. (11) is independent of the kinetic energy $\tilde{\varepsilon}_k$, and it rotates the spin around the y axis by an angle γ, also independent of q. By changing the strength of the SOI or the distance between the junctions, according to Eq. (12), the values of γ can be varied from 0 up to 2π. Once we fix the rotation angle γ (e.g., $\gamma=\pi/2$ as in Fig. 3, bottom), we can design the gate by fixing d (if we assume a InGaAs device with the SOI strength near the natural value we obtain $d \sim L_{so}/4 \sim 100$ nm).

In the language of quantum informatics,[33] the transformation discussed above represents a rather general single-qubit gate. A transformation of the form $\mathbf{U}$ with $\gamma=\pi/2$ is essentially a so-called quantum NOT gate, which plays a distinguished role in quantum algorithms. Moreover we note that in principle a number of other gates can be constructed by coupling several of those Π junctions.

If we take into account the presence of a Dresselhaus term of SOI, the unitary matrix reported in Eq. (11) has to be replaced by a more general matrix—once again unitary. The matrix elements of U are $u_{11}=-u^{*}22=\cos(\gamma) + i\cos(\lambda)\sin(\gamma)$ and $u_{21}=u_{12}=i\sin(\lambda)\sin(\gamma)$ with $\lambda=\frac{\pi}{2}-2\bar{\theta}$. However, the important fact is that U is a unitary matrix and thus is able to perform a nontrivial spin transformation in the qubit space.

VII. DISCUSSION

In this paper we discussed some realistic or theoretical devices capable of acting as spintronic gates based on the Rashba SOI. We analyzed an idealized model system in which transport is in the CB regime, characterized by the fact that just one single electron tunnels at the time through the QD, and the system was treated as being one dimensional, i.e., the finite width, W, of the wire was not included in the calculation. This corresponds to assuming 1 degree of freedom to be frozen because the energy $\hbar\omega=\frac{h^2}{2m^{*}W^2}$ is larger than both the energy Δ and the thermal energy $k_B T$. The results we have shown were obtained using values of the well width within those given by presently available 2DEGs and nanolithography techniques; in fact, the lithographical width of a wire defined in a 2DEG can be as small as 20 nm (Ref. 34) ($\hbar\omega \sim 50$ meV). Larger values of the QW's width yield a reduction in the intersubband gap so that for $W=50$ nm one has $\hbar\omega \sim 8$ meV. In this case the excitation gap Δ (i.e., the difference between the ground state and the first excited level) becomes comparable with the intersubband gap; hence the Q1D approximation can fail.

Here we proposed conductors smaller than the dephasing length for low temperatures. In fact, phase coherence and spin coherence lengths[35] have been found to have values up to 100 mm, while recently it was found that the finite width of the wires has a small effect on the loss of coherence of the spin state.

The SOI strengths, which were shortly discussed above, have been theoretically evaluated for some semiconductor compounds.[36] In a QW patterned in InGaAs/InP heterostructures,[6,15] the natural values read $\alpha \gtrsim 10^{-10}$ eV m while for GaAs-AsGaAl interfaces, one typically observes[16] values of $\alpha \sim 10^{-11}$ eV m, whereas for HgTe-based heterostructures α can be more than three times larger.[37] Thus, values of k_R up to $\sim 10^{-2}$ nm^{-1} can be assumed due to the natural SOI, i.e., to the structure inversion asymmetry of the heterostructure quantum well. On the contrary, larger values have to be obtained by controlling the transverse electric field, e.g., by tuning the voltage on the gate electrode. We also want to point out that the excitation gap Δ is much larger than the thermal energy provided that $T \lesssim 10$ K.

In conclusion, we have shown that a quantum Π nanojunction with Rashba-type SOI can serve as a one-qubit quantum gate for electron spins. The spin transformation properties of the gates can be extended by coupling such nanojunctions in series. Different types of gates can be realized by tuning the electric-field strength and changing the geometric position of the two cross junctions. The considered parameters are within the experimentally feasible range.

We acknowledge the support of the grant 2006 PRIN "Sistemi Quantistici Macroscopici-Aspetti Fondamentali ed Applicazioni di strutture Josephson Non Convenzionali."

[1] D. D. Awschalom, D. Loss, and N. Samarth, *Semiconductor Spintronics and Quantum Computation* (Springer, Berlin, 2002); B. E. Kane, Nature (London) **393**, 133 (1998).
[2] S. A. Wolf, D. D. Awschalom, R. A. Buhrman, J. M. Daughton, S. von Molnar, M. L. Roukes, A. Y. Chtchelkanova, and D. M. Treger, Science **294**, 1488 (2001).
[3] L. D. Landau and E. M. Lifshitz, *Quantum Mechanics* (Pergamon, Oxford, 1991).
[4] M. J. Kelly, *Low-Dimensional Semiconductors: Material, Physics, Technology, Devices* (Oxford University Press, Oxford, 1995).
[5] Yu. A. Bychkov and E. I. Rashba, Pis'ma Zh. Eksp. Teor. Fiz. **39**, 66 (1984) [JETP Lett. **39**, 78 (1984)].
[6] A. V. Moroz and C. H. W. Barnes, Phys. Rev. B **61**, R2464 (2000).
[7] S. Datta and B. Das, Appl. Phys. Lett. **56**, 665 (1990).
[8] G. Dresselhaus, Phys. Rev. **100**, 580 (1955).
[9] S. D. Ganichev, V. V. Belkov, L. E. Golub, E. L. Ivchenko, P. Schneider, S. Giglberger, J. Eroms, J. De Boeck, G. Borghs, W. Wegscheider, D. Weiss, and W. Prettl, Phys. Rev. Lett. **92**, 256601 (2004).
[10] B. Das, S. Datta, and R. Reifenberger, Phys. Rev. B **41**, 8278 (1990).
[11] J. Luo, H. Munekata, F. F. Fang, and P. J. Stiles, Phys. Rev. B **41**, 7685 (1990).
[12] T. Hassenkam, S. Pedersen, K. Baklanov, A. Kristensen, C. B. Sorensen, P. E. Lindelof, F. G. Pikus, and G. E. Pikus, Phys. Rev. B **55**, 9298 (1997).
[13] G. Engels, J. Lange, Th. Schäpers, and H. Lüth, Phys. Rev. B **55**, R1958 (1997).
[14] M. Schultz, F. Heinrichs, U. Merkt, T. Colin, T. Skauli, and S. Løvold, Semicond. Sci. Technol. **11**, 1168 (1996).
[15] D. Grundler, Phys. Rev. Lett. **84**, 6074 (2000).
[16] J. Nitta, T. Akazaki, H. Takayanagi, and T. Enoki, Phys. Rev. Lett. **78**, 1335 (1997).
[17] H. L. Stormer, Z. Schlesinger, A. Chang, D. C. Tsui, A. C. Gossard, and W. Wiegmann, Phys. Rev. Lett. **51**, 126 (1983).
[18] J. Könemann, R. J. Haug, D. K. Maude, V. I. Fal'ko, and B. L. Altshuler, Phys. Rev. Lett. **94**, 226404 (2005).
[19] Y. Ohno, D. K. Young, B. Beschoten, F. Matsukura, H. Ohno, and D. D. Awschalom, Nature (London) **402**, 790 (1999).
[20] J. M. Kikkawa, I. P. Smorchkova, N. Samarth, and D. D. Awschalom, Science **277**, 1284 (1997); J. M. Kikkawa and D. D. Awschalom, Phys. Rev. Lett. **80**, 4313 (1998); D. D. Awschalom and J. M. Kikkawa, Phys. Today **52**(6), 33 (1999).
[21] J. A. Gupta, R. Knobel, N. Samarth, and D. D. Awschalom, Science **292**, 2458 (2001).
[22] L. P. Kouwenhoven, G. Schoön, and L. L. Sohn, in *Mesoscopic Electron Transport*, NATO Advanced Study Institute, Series E: Applied Science, edited by L. L. Sohn, L. P. Kouwenhoven, and G. Schön (Kluwer Academic, Dordrecht, 1997), Vol. 345.
[23] M. König, A. Tschetschetkin, E. M. Hankiewicz, J. Sinova, V. Hock, V. Daumer, M. Schäfer, C. R. Becker, H. Buhmann, and L. W. Molenkamp, Phys. Rev. Lett. **96**, 076804 (2006).
[24] S. Bellucci and P. Onorato, Phys. Rev. B **77**, 165305 (2008).
[25] P. Foldi, B. Molnar, M. G. Benedict, and F. M. Peeters, Phys. Rev. B **71**, 033309 (2005).
[26] J. G. Williamson, A. A. M. Staring, L. P. Kouwenhoven, H. van Houten, C. W. J. Beenakker, C. E. Timmering, M. Mabesoone, and C. T. Foxon, *Lateral Electron Transport Through a Quantum Dot: Coulomb Blockade and Quantum Transport*, in Nanostructures and Mesoscopic Systems, Proceedings of the International Symposium, Santa Fe, New Mexico, 1991, edited by W. P. Kirk and M. A. Reed (Academic Press, San Diego, 1992).
[27] S. E. Laux, D. J. Frank, and F. Stern, Surf. Sci. **196**, 101 (1988); H. Drexler, W. Hansen, S. Manus, J. P. Kotthaus, M. Holland, and S. P. Beaumont, Phys. Rev. B **49**, 14074 (1994); B. Kardynał, C. H. W. Barnes, E. H. Linfield, D. A. Ritchie, J. T. Nicholls, K. M. Brown, G. A. C. Jones, and M. Pepper, *ibid.* **55**, R1966 (1997).
[28] M. Governale and U. Zulicke, Phys. Rev. B **66**, 073311 (2002).
[29] S. Bellucci and P. Onorato, Phys. Rev. B **68**, 245322 (2003).
[30] J. B. Xia, Phys. Rev. B **45**, 3593 (1992); P. S. Deo and A. M. Jayannavar, *ibid.* **50**, 11629 (1994).
[31] S. Griffith, Trans. Faraday Soc. **49**, 345 (1953); **49**, 345 (1953).
[32] S. Bellucci and P. Onorato, Phys. Rev. B **71**, 075418 (2005).
[33] M. A. Nielsen and I. L. Chuang, *Quantum Computation and Quantum Information* (Cambridge University Press, Cambridge, 2000).
[34] M. Knop, M. Richter, R. Maßmann, U. Wieser, U. Kunze, D. Reuter, C. Riedesel, and A. D. Wieck, Semicond. Sci. Technol. **20**, 814 (2005).
[35] J. M. Kikkawa and D. D. Awschalom, Phys. Rev. Lett. **80**, 4313 (1998).
[36] E. A. de Andrada e Silva, G. C. La Rocca, and F. Bassani, Phys. Rev. B **55**, 16293 (1997).
[37] X. C. Zhang, A. Pfeuffer-Jeschke, K. Ortner, V. Hock, H. Buhmann, C. R. Becker, and G. Landwehr, Phys. Rev. B **63**, 245305 (2001).